Molecules and Cells

Knockdown of lncRNA *PVT1* Inhibits Vascular Smooth Muscle Cell Apoptosis and Extracellular Matrix Disruption in a Murine Abdominal Aortic Aneurysm Model

Zhidong Zhang[1,2], Gangqiang Zou[1,2], Xiaosan Chen[1,2], Wei Lu[1,2], Jianyang Liu[1,2], Shuiting Zhai[1,3], and Gang Qiao[1,2,*]

[1]Department of Vascular and Endovascular Surgery, Henan Provincial People's Hospital, Henan, China, [2]Department of Aortic Surgery, [3]Department of Vascular and Endovascular Surgery, Fuwai Central China Cardiovascular Hospital, Henan, China
*Correspondence: gangqiao2004@126.com
http://dx.doi.org/10.14348/molcells.2018.0162
www.molcells.org

This study was designed to determine the effects of the long non-coding RNA (lncRNA) plasmacytoma variant translocation 1 (*PVT1*) on vascular smooth muscle cell (VSMC) apoptosis and extracellular matrix (ECM) disruption in a murine abdominal aortic aneurysm (AAA) model. After injection of *PVT1*-silencing lentiviruses, AAA was induced in Apolipoprotein E-deficient ($ApoE^{-/-}$) male mice by angiotensin II (Ang II) infusion for four weeks. After Ang II infusion, mouse serum levels of pro-inflammatory cytokines were analysed, and aortic tissues were isolated for histological, RNA, and protein analysis. Our results also showed that *PVT1* expression was significantly upregulated in abdominal aortic tissues from AAA patients compared with that in controls. Additionally, Ang II treatment significantly increased *PVT1* expression, both in cultured mouse VSMCs and in AAA murine abdominal aortic tissues. Of note, the effects of Ang II in facilitating cell apoptosis, increasing matrix metalloproteinase (MMP)-2 and MMP-9, reducing tissue inhibitor of MMP (TIMP)-1, and promoting switching from the contractile to synthetic phenotype in cultured VSMCs were enhanced by overexpression of *PVT1* but attenuated by knockdown of *PVT1*. Furthermore, knockdown of *PVT1* reversed Ang II-induced AAA-associated alterations in mice, as evidenced by attenuation of aortic diameter dilation, marked adventitial thickening, loss of elastin in the aorta, enhanced aortic cell apoptosis, elevated MMP-2 and MMP-9, reduced TIMP-1, and increased pro-inflammatory cytokines. In conclusion, our findings demonstrate that knockdown of lncRNA *PVT1* suppresses VSMC apoptosis, ECM disruption, and serum pro-inflammatory cytokines in a murine Ang II-induced AAA model.

Keywords: abdominal aortic aneurysm, apoptosis, extracellular matrix, lncRNA PVT1, vascular smooth muscle cell

INTRODUCTION

Abdominal aortic aneurysm (AAA) is defined as focal dilatations of the abdominal aorta that are either 50% greater than the proximal normal segment or when the aorta measures more than 30 mm in diameter (Kumar et al., 2017). AAA is a leading cause of sudden death in the elderly (Ren et al., 2015). The risk factors of AAA include male gender, age of more than 75 years, prior vascular disease, hypertension, hypercholesterolaemia, cigarette smoking, and family history (Pande and Beckman, 2008). Clinically, surgical

Received 11 April, 2018; revised 8 October, 2018; accepted 15 October, 2018; published online 1 February, 2019

eISSN: 0219-1032

intervention is only recommended when the aneurysms are prone to rupture (Kent, 2014). Unfortunately, there is a lack of effective therapeutic drugs to limit the progression of AAA (Zhou et al., 2017). Therefore, basic research concerning the molecular mechanism of AAA is urgently needed to identify new biomarkers and therapeutic targets.

AAA is characterized by extracellular matrix (ECM) degradation, loss of arterial wall integrity, apoptosis of vascular smooth muscle cells (VSMCs), and infiltration of inflammatory cells (Miyake and Morishita, 2009). Previous studies suggest that apoptosis and depletion of VSMCs make an important contribution to AAA by eliminating a cell population that promotes connective tissue repair (Sachdeva et al., 2017). In addition, studies of human AAA tissues have shown that extensive inflammatory infiltrates containing macrophages, lymphocytes, and mast cells occurred in both the media and adventitia and that increased aneurysm diameter was associated with a higher density of inflammatory cells in the adventitia (Freestone et al., 1995). These infiltrating cells secrete various inflammatory cytokines, such as tumour necrosis factor (TNF)-α, interleukin (IL)-1β, and IL-6. These cytokines can induce the activation of matrix metalloproteinases (MMPs), particularly MMP-2 and MMP-9 (Galis et al., 1995; Sakata et al., 2000). MMPs and their tissue inhibitors (TIMPs) play a crucial role in ECM metabolism (Kosmala et al., 2008). Increased expression of MMPs and decreased expression of TIMPs contribute to ECM disruption and VSMC depletion, leading to AAA progression and rupture (Li and Maegdefessel, 2017). In addition, AAA demonstrates VSMCs phenotypic modulation of VSMCs characterized by downregulation of contractile-phenotype VSMC biomarkers (for example, α-smooth muscle actin [α-SMA]), upregulation of synthetic biomarkers (for example, osteopontin [OPN]), and upregulation of MMPs (Ailawadi et al., 2009; Sachdeva et al., 2017). Collectively, targeting ECM degradation, vascular apoptosis, and vascular inflammation may be a potential therapeutic approach for AAA pathologies.

Long noncoding RNAs (lncRNAs) are a class of transcripts longer than 200 nucleotides that are transcribed by RNA polymerase II, polyadenylated, spliced, and capped but lack significant open reading frames and cannot encode proteins (Ng et al., 2013). Collective evidence indicates that lncRNAs exert a wide variety of biological functions through various mechanisms and are correlated with both normal developmental processes and diseases such as cancer (Kung et al., 2013). Nevertheless, studies of the involvement of lncRNAs in AAA remain scarce (Yang et al., 2016; Zhou et al., 2017). Plasmacytoma variant translocation 1 (*PVT1*) is a newly discovered lncRNA that functions as an oncogenic molecule in diverse cancer types, such as gastrointestinal cancers (Liu et al., 2017), cervical cancer (Shen et al., 2017), pancreatic cancer (Zhao et al., 2018), and non-small cell lung cancer (NSCLC) (Wu et al., 2017). However, the role of *PVT1* in AAA is less understood.

PVT1 was upregulated more than 3-fold in AAA tissues compared with normal tissue in a microarray analysis (Yang et al., 2016), indicating that *PVT1* is closely related to the pathology of AAA. Recently, Chen et al. (Chen et al., 2017) proposed that, in NSCLC cell lines A549 and 95D, *PVT1* facilitated invasion by upregulating MMP-9, a protein closely related to ECM degradation. Hence, we speculated that lncRNA *PVT1* can promote the expression of MMP-9 and facilitate ECM degradation, leading to VSMC apoptosis and thus to the formation of AAA.

MATERIALS AND METHODS

Patients and tissue samples

AAA patients (n = 20) and control subjects (n = 20, aged 55-80 years) were recruited from Henan Provincial People's Hospital. AAA tissues were acquired by surgery, and normal abdominal aortic tissues were obtained from subjects who suffered physical trauma unrelated to AAA. AAA and normal aortic tissues from each participant were snap-frozen in liquid nitrogen immediately after resection and stored at -80℃. This study was approved by the Research Ethics Committee of Henan Provincial People's Hospital, and a written informed consent was obtained from each participant (Approval Number: HNPPH-2016-23).

RNA isolation and quantitative real-time reverse transcription PCR (qRT-PCR)

qRT-PCR was performed as previously described (Guo et al., 2018), with some modifications. Total RNA from VSMCs or tissues was isolated using TRIzol (Invitrogen, Canada) reagent according to the standard protocol. First-strand cDNA was synthesized using the Reverse Transcription System Kit (Takara, China). qRT-PCR was performed using SYBR Green Mixture (Takara) in the ABI StepOne-Plus System (Applied Biosystems, USA). Data were normalized to the internal control, GAPDH. Comparative quantification was determined using the $2^{-\Delta\Delta Ct}$ method.

Cell culture

Mouse primary VSMCs were purchased from Procell Co., China (cat. no. CP-M076). VSMCs were maintained in complete Dulbecco's modified Eagle's medium (DMEM, Gibco BRL, USA), supplemented with 10% foetal bovine serum (FBS, Gibco BRL), penicillin (100 U/mL) and streptomycin (100 mg/mL) in humidified air with 5% CO_2 at 37℃.

Generation of lncRNA-PVT1 overexpression and knockdown cells

Generation of lncRNA-*PVT1* overexpressed cells was performed as previously described (Chen et al., 2017). In brief, full-length human lncRNA-*PVT1* cDNA was cloned into the pCMV vector. VSMCs were transfected with the empty pCMV (OE-Ctrl) or pCMV-lncRNA-*PVT1* vectors. Stable cells were selected with 600 mg/mL G418 for 1 week.

Short hairpin RNAs (shRNAs) against lncRNA-*PVT1* were designed as previously described (Chen et al., 2017). The sequences of lncRNA-*PVT1* were provided as follows: 5′-CCUGCAUAACUAUCUGCUUTT-3′. shRNAs were cloned into shRNA lentiviral vector pLKO.1. Production of lentiviral particles was conducted according to standard protocols. VSMCs were transfected with lentiviral constructs for 24 h with 2 mg/mL polybrene (Sigma-Aldrich, USA). Forty-eight hours later, stable VSMCs were selected with 1 mg/mL

puromycin for 1 week. The cells were collected 48 h post-transduction for qRT-PCR to determine the transfection efficiency.

Animals

Apolipoprotein E-deficient (ApoE$^{-/-}$) male mice (genetic C57BL/6J background, 6-8 weeks old, 20-25 g) were purchased from Shanghai Slac Laboratory Animal Co, Ltd (China). All mice were raised in a specific pathogen-free environment under a 12 h light/12 h dark cycle throughout the experimental period. All animal experiments were performed in strict accordance with the guidelines for the Care and Use of Laboratory Animals of the National Institutes of Health and approved by the Animal Care and Use Committee of Henan Provincial People's Hospital (Approval Number: HNPPH-2017-13).

AAA model and treatment

Angiotensin II (Ang II) was used to induce AAA model in ApoE$^{-/-}$ mice in this study. Male ApoE$^{-/-}$ mice were infused with 1000 ng/kg/min Ang II (Sigma-Aldrich) over the course of 28 days. Ang II was infused via a subcutaneous osmotic minipump (Alzet Osmotic Pump, Model 2004; Durect Corp, USA) as previously described (Qin et al., 2017). Mice were anaesthetized with isoflurane as previously described, and pumps were implanted subcutaneously in the back in the prone position through a small incision that was closed with sutures (Fu et al., 2013).

The ApoE$^{-/-}$ male mice were randomly divided into four groups: normal saline (NS), Ang II, Ang II + sh-Ctrl, and Ang II + sh-*PVT1* groups. Mice in the Ang II + sh-Ctrl and Ang II + sh-*PVT1* groups received an injection of lentivirus carrying sh-Ctrl and sh-*PVT1* gene (1×10^{11} plaque-forming unit [pfu]/mouse) via the tail vein, respectively. Mice in the NS and Ang II groups were injected with equal volumes of NS. Four weeks after lentivirus injection, mice in the Ang II, Ang II + sh-Ctrl, and Ang II + sh-*PVT1* groups received Ang II infusion via a subcutaneous osmotic minipump, as described above. Mice in the NS group received an injection of an equal volume of NS. At day 0, 7, 14, 21, and 28 post-Ang II infusion, B-mode ultrasound imaging was conducted to measure the aortic diameters of the mice in each group as previously described (Maegdefessel et al., 2012). Mice were sacrificed four weeks after Ang II infusion. Aortic tissues were isolated and then stored at -80℃ for histological, RNA, and protein analysis. The blood samples were collected to separate the serum for cytokine detection.

Cell apoptosis assay

To quantify rate of apoptosis, an annexin V-fluorescein isothiocyanate (FITC)/propidium iodide (PI) cell apoptosis kit was used according to the manufacturer's instructions (Invitrogen). In brief, 48 h post-transfection, VSMCs were incubated with 10 μM Ang II for an additional 48 h. The total cells were washed twice with PBS buffer (pH 7.4), and re-suspended in the staining buffer provided in the kit. Subsequently, 5 μL Annexin V/FITC and 5 μL PI were mixed with VSMCs. After 10 min of cultivation at room temperature, the mixtures were analysed using the FACScan flow cytometry (BD Biosciences, USA). The percentage of apoptotic cells is indicated by the sum of the numerical values represented in the upper right and lower right quadrants. The cell apoptosis rate is equivalent to the average apoptosis rate from five flow cytometry analyses.

Western blot

Protein was isolated from VSMCs or aortic tissues using a RIPA lysis buffer kit (Santa Cruz Biotechnology, Inc., USA). The protein content was determined in the supernatants using a Bio-Rad protein assay (Bio-Rad Laboratories, Inc., USA). Protein lysates (30 μg/sample) were separated on 10% SDS-PAGE and transferred to polyvinylidene difluoride (PVDF, Millipore Corp., USA) membranes. The membranes were blocked in 5% fat-free milk overnight at 4℃. Membranes were then probed with the following primary antibodies purchased from Abcam (Cambridge, USA): anti-α-SMA (cat. no. ab5694, 1:1,000), anti-OPN (cat. no. ab8448, 1:1,000), anti-MMP-2 (cat. no. ab92536, 1:1,000), anti-MMP-9 (cat.no. ab38898, 1:1,000), and anti-TIMP-1 (cat. no. ab38978, 1:1,000) and incubated overnight at 4℃. Subsequently, protein bands were detected by incubation with horseradish peroxidase-conjugated goat anti-mouse immunoglobulin G (IgG, cat. no. ab6789; 1:2,000; Abcam) at room temperature for 1 h. Signals were detected using an enhanced chemiluminescence kit (ECL kit, Wuhan Boster Biotechnology Co., Ltd, China) and exposed to Kodak X-OMAT film (Kodak, Rochester, USA). The band intensity was quantified with the Quantity One software. Each experiment was performed at least three times. GAPDH served as the loading control.

Histological analysis

The abdominal aortas of the mice in each group were cut and fixed in 4% paraformaldehyde for 24 h, dehydrated, embedded in paraffin and cut into serial sections (6 μm thick). Sections were stained with haematoxylin and eosin (HE) and Elastica van Gieson (EVG) as previously described (Watanabe et al., 2014). Immunohistochemistry for MMP-2 and MMP-9 was performed as previously described (Martorell et al., 2016). In brief, a rabbit polyclonal anti-mouse MMP-2 (cat. no. ab37150, 1:100, Abcam) or an anti-mouse MMP-9 (cat. no. ab38898, 1:100, Abcam) antibody was used. Representative images were captured using a fluorescence microscope (Nikon Corporation, Japan).

In situ detection of apoptotic cells

Apoptotic cells in the aortic tissues were detected by TUNEL (terminal deoxynucleotidyl transferase dUTP nick end labelling) staining, according to the manufacturer's protocol for the *In Situ* Cell Death Detection kit (Roche Diagnostics, GmbH, Germany). Apoptotic cells were imaged under a fluorescence microscope (Nikon Corporation). The TUNEL-positive cells were counted in 10 randomly selected high-power fields (scale bar: 20 μm). The apoptosis index was calculated as previously described (3).

Cytokine measurement

Cytokine (TNF-α, IL-1β, and IL-6) levels were determined by

enzyme-linked immunosorbent assay (ELISA) according to the manufacturer's protocol for each ELISA kit (Bender MedSystems, Austria).

Statistical analysis

Statistical analyses were performed using SPSS statistical software package standard version 16.0 (SPSS, Inc., USA). Statistical differences between two independent groups were determined using Student's *t*-test. For multiple groups, the statistical analyses were performed by one-way analysis of variance (ANOVA) followed by Tukey's test. Data were expressed as the mean ± standard deviation (SD). Experiments were performed in triplicate. $P < 0.05$ indicates statistically significant differences.

RESULTS

Increased PVT1 expression in abdominal aortic tissues from AAA patients and ApoE$^{-/-}$ AAA model mice

To investigate the correlation between *PVT1* and AAA, we performed qRT-PCR to detect relative *PVT1* expression in abdominal aortic tissues from AAA patients and ApoE$^{-/-}$

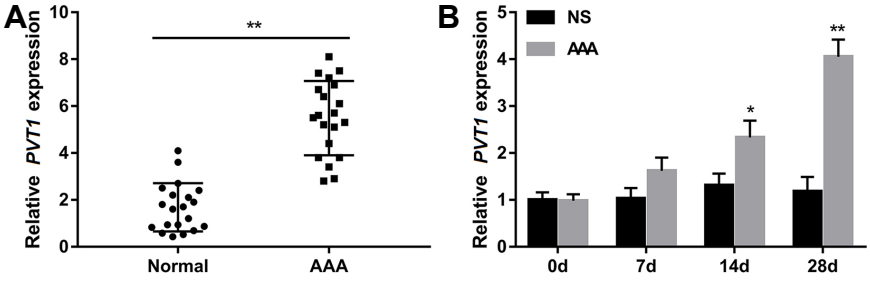

Fig. 1. lncRNA *PVT1* was upregulated in abdominal aortic tissues from AAA patients and ApoE$^{-/-}$ AAA models. (A) qRT-PCR was performed to detect relative *PVT1* expression in AAA tissues and normal abdominal aortic tissues. Each circle and block represents an individual subject. n=20 for each group. $^{**}P < 0.01$ *vs.* normal group. (B) Male ApoE$^{-/-}$ mice were infused with Ang II (1000 ng/kg/min) for 28 days to induce AAA. Relative *PVT1* expression was significantly upregulated in the abdominal aortas from Ang II-treated mice at days 14 and 28 compared with mice that received an equal volume of NS. N = 5 for each time point. $^{*}P < 0.05$, $^{**}P < 0.01$ *vs.* NS group. AAA: abdominal aortic aneurysm; NS: normal saline; Ang II: Angiotensin II; ApoE$^{-/-}$: apolipoprotein E-deficient.

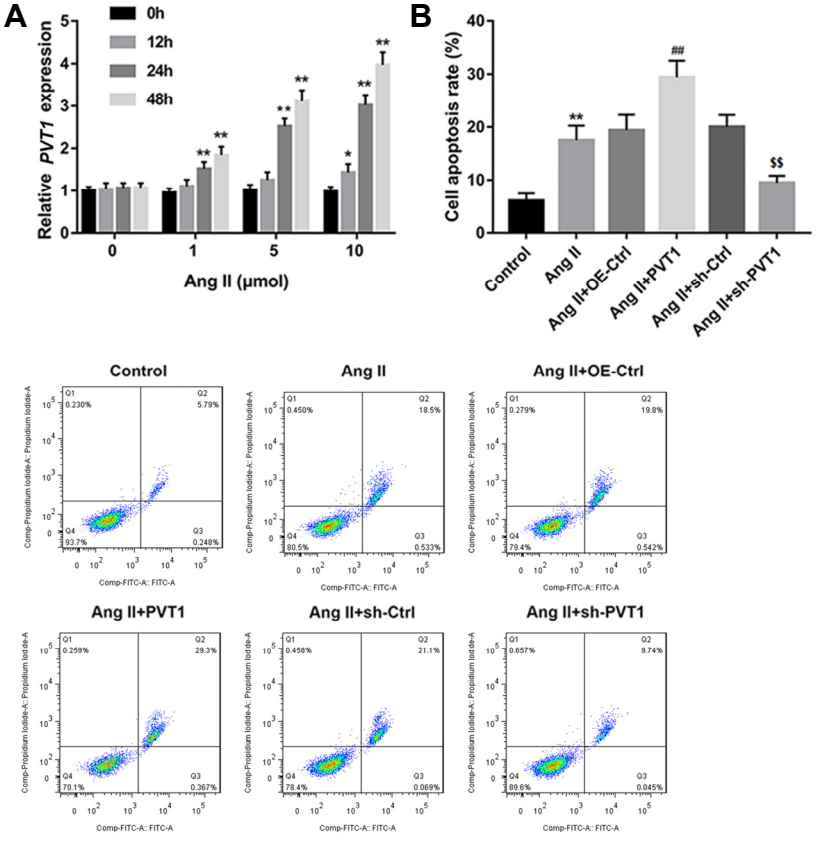

Fig. 2. Relative *PVT1* expression in Ang II-induced VSMCs and the effect of *PVT1* expression on Ang II-induced apoptosis. (A) Relative *PVT1* expression was detected by qRT-PCR in cultured mouse primary VSMCs that were stimulated with different concentrations of Ang II (0, 1, 5, and 10 μM) at various time points (0, 12, 24, and 48 h). $^{*}P < 0.05$, $^{**}P < 0.01$ *vs.* 0 h group. The cultured VSMCs were then induced with Ang II (10 μM, 48 h) alone or transfected with the indicated vectors. (B) The apoptosis rate of cultured VSMCs was examined by flow cytometry. A representative flow cytometry plot of cultured VSMCs from each group is shown. $^{**}P < 0.01$ *vs.* control group, $^{\#\#}P < 0.01$ *vs.* Ang II+OE-Ctrl group, $^{\$\$}P < 0.01$ *vs.* Ang II+sh-Ctrl group. Ang II: Angiotensin II; OE-Ctrl: overexpression control; *PVT1*: *PVT1* overexpression.

AAA models. Data revealed that the expression of *PVT1* in AAA tissues was significantly higher than that in normal abdominal aortic tissues (Fig. 1A). In addition, ApoE$^{-/-}$ mice expressed significantly higher levels of *PVT1* at days 14 and 28 after Ang II (1000 ng/kg/min) infusion than did mice receiving an equal volume of saline (Fig. 1B). These results suggested an association between PVT1 expression and AAA.

PVT1 is increased in Ang II-induced VSMCs

Next, we examined relative *PVT1* expression in mouse cultured VSMCs induced by Ang II, which was shown to induce AAA formation. Mouse primary VSMCs were cultured with various concentrations of Ang II (0, 1, 5, and 10 μM) for 0, 12, 24, and 48 h. The data revealed that, compared to the 0 h group, expression of *PVT1* in Ang-II-treated VSMCs was elevated with increasing concentration and time (Fig. 2A). Because 10 μM of Ang II treatment for 48 h resulted in the highest level of *PVT1* expression, we used these conditions in the subsequent experiments.

Effects of PVT1 expression on apoptosis, ECM disruption and phenotype switching of Ang II-induced VSMCs

To explore the effect of *PVT1* expression on cell apoptosis and ECM degradation in Ang II-induced VSMCs, we overexpressed and knocked down *PVT1* in cultured VSMCs. Data demonstrated that Ang II treatment alone significantly increased cell apoptosis rate of VSMCs compared to that of the control group. In addition, the induction of apoptosis in Ang II-treated VSMCs was significantly enhanced by overexpression of *PVT1* but diminished by knockdown of *PVT1* (Fig. 2B). We then examined the effects of *PVT1* expression on ECM degradation and phenotypic switching in VSMCs. Western blot analysis revealed that compared with the control group, Ang II treatment alone increased protein levels of MMP-2 and MMP-9 but decreased levels of the inhibitor TIMP-1, indicating the contribution of Ang II to ECM degradation in cultured VSMCs. Furthermore, the protein level of α-SMA, a biomarker of contractile VSMCs, was suppressed, and that of OPN, another biomarker of synthetic VSMCs, was upregulated by Ang II treatment alone in comparison with the control group. These results suggested that Ang II treatment promoted phenotypic switching from the contractile to synthetic state in VSMCs. Notably, the effect of Ang II on ECM degradation and phenotype switching in VSMCs was enhanced by overexpression of *PVT1* but reversed by knockdown of *PVT1* (Figs. 3A and 3B).

sh-PVT1 attenuates Ang II-induced AAA formation in ApoE$^{-/-}$ mice

To assess the potential role of *PVT1* as a mediator of AAA, mice were infused with Ang II (1000 ng/kg/min) for 28 days at week 4 after injection of *PVT1*-silencing lentiviruses. At days 0, 7, 14, 21, and 28 post-Ang II infusion, the maximal

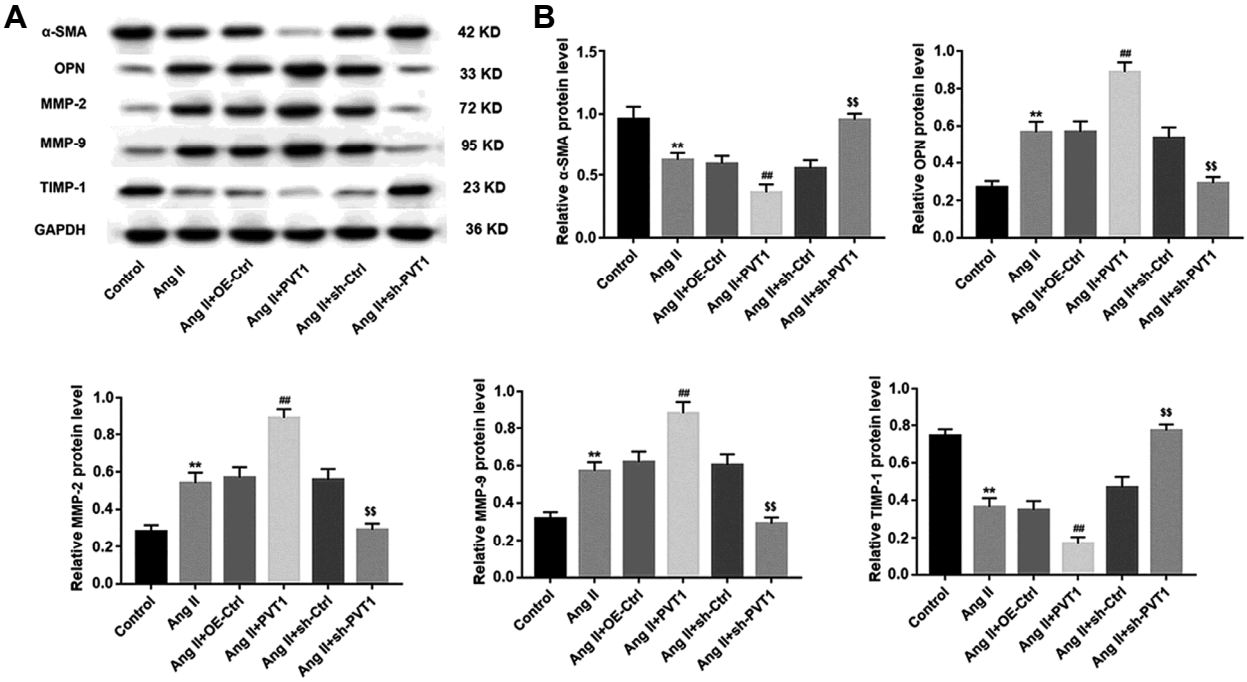

Fig. 3. Effects of *PVT1* expression on ECM degradation and phenotype switching of Ang II-induced VSMCs. (A) The protein levels of α-SMA, OPN, MMP-2, MMP-9, and TIMP-1 in cultured VSMCs in each group were examined by Western blot. GAPDH served as the loading control. (B) Quantification for all Western blots. $^{**}P < 0.01$ *vs.* control group, $^{\#\#}P < 0.01$ *vs.* Ang II+OE-Ctrl group, $^{\$\$}P < 0.01$ *vs.* Ang II+sh-Ctrl group. Ang II: Angiotensin II; OE-Ctrl: overexpression control; *PVT1*: *PVT1* overexpression; α-SMA: α-smooth muscle actin; OPN: osteopontin; MMP-2: matrix metalloproteinase-2; MMP-9: matrix metalloproteinase-9; TIMP-1: tissue inhibitors of metalloproteinase-1.

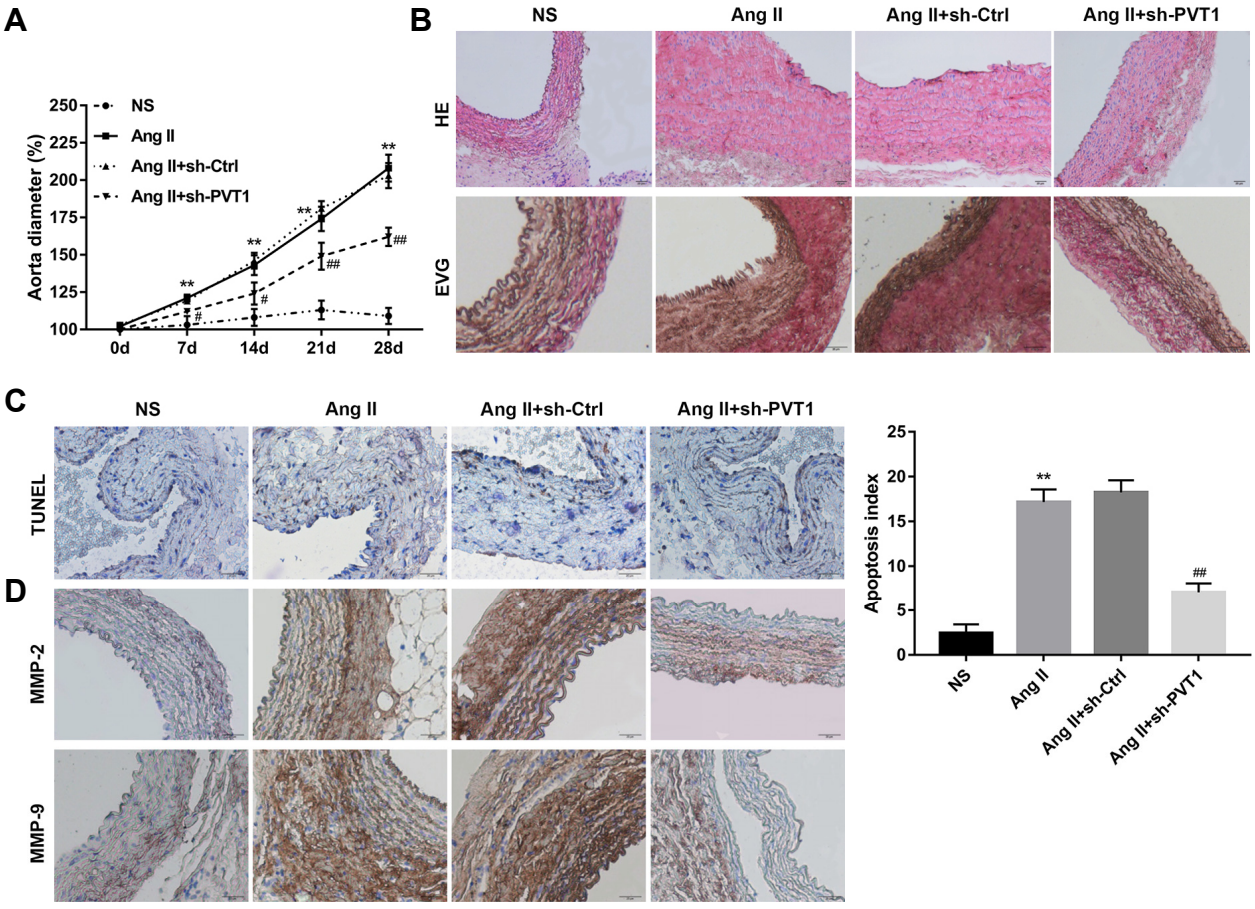

Fig. 4. sh-*PVT1* attenuated Ang II-induced AAA in mice. (A) Male ApoE$^{-/-}$ mice were randomly divided into four groups: NS, Ang II, Ang II + sh-Ctrl, and Ang II + sh-PVT1 groups. At days 0, 7, 14, 21, and 28 post-Ang II infusion, B-mode ultrasound imaging was conducted to measure the maximal external diameter of the abdominal aorta of the mice in each group. n=15 in each group. (B) Paraffin-embedded sections of abdominal aortas were stained with HE and EVG to evaluate the changes in aortic tissue structure and the damage of arterial wall elastic fibres, respectively. (C) TUNEL staining was performed to assess aortic cell apoptosis. The TUNEL-positive (brown) cells were counted in 10 randomly selected high-power fields, and the apoptosis index was calculated. (D) Representative images of immunohistochemical staining for MMP-2 and MMP-9 in each group. Scale bar: 20 μm. n=15 for each group. $^{**}P < 0.01$ *vs.* NS group, and $^{\#}P < 0.05$, $^{\#\#}P < 0.01$ *vs.* Ang II+sh-Ctrl group. NS: normal saline; Ang II: Angiotensin II; HE: haematoxylin and eosin; EVG: Elastica van Gieson; TUNEL: terminal deoxynucleotidyl transferase dUTP nick end labelling; MMP-2: matrix metalloproteinase-2; MMP-9: matrix metalloproteinase-9.

external diameter of the abdominal aorta from each mouse was measured. The data revealed that, compared to that in the NS group, the maximal external diameter of the abdominal aorta from mice in the Ang II group was significantly larger after Ang II infusion and increased over time. However, sh-*PVT1* treatment significantly reduced this aortic dilation (Fig. 4A).

Four weeks after Ang II infusion, the abdominal aortas of the mice in each group were isolated and cut into serial sections. HE staining revealed modest thinning of the media and marked thickening of the adventitia in the Ang II group compared to the NS group; however, these changes were attenuated by treatment with sh-*PVT1*. Fragmentation of elastin in the aortic wall is one of the most important steps in the development of human and animal AAA (Qin et al., 2017). EVG staining showed the wavy structure of the elastic lamellae in the NS group, which was disrupted and degraded in the Ang II-treated group, indicating ECM degradation. Treatment with sh-*PVT1* inhibited this fragmentation and preserved the elastin structure of the aorta (Fig. 4B). Furthermore, TUNEL staining showed there was greater aortic cell apoptosis in the abdominal aortas in the Ang II group than in the NS group. Treatment with sh-*PVT1* significantly diminished Ang II-induced aortic cell apoptosis (Fig. 4C). In addition, immunohistochemistry for MMP-2 and MMP-9 revealed that Ang II infusion significantly enhanced expression of MMP-2 and MMP-9, indicating the promotion of Ang II in ECM degradation. However, these changes were attenuated by sh-*PVT1* treatment (Fig. 4D). These results showed that sh-*PVT1* treatment inhibited the progressive

dilation of the aorta, maintained ECM structure, and suppressed the activity of MMPs and aortic cell apoptosis, indicating the importance of *PVT1* in the formation of AAA in mice.

sh-PVT1 attenuates Ang II-induced PVT1 expression, ECM degradation, and inflammation in ApoE$^{-/-}$ mice

Four weeks after Ang II infusion, aortic tissues were isolated from mice and then stored at -80℃ for RNA and protein analysis. The data revealed that Ang II infusion significantly upregulated *PVT1* expression compared to the NS group. However, sh-*PVT1* treatment significantly reduced Ang II-induced *PVT1* expression (Fig. 5A). In addition, Western blot analysis confirmed the expression patterns of MMP-2 and MMP-9 as revealed by immunohistochemistry. Sh-*PVT1* treatment reversed the upregulation of MMP-1 and MMP-9 protein expression as well as the downregulation of TIMP-1 mediated by Ang II infusion, bringing them to levels comparable to those of the NS group (Fig. 5B) and further supporting the role *PVT1* in ECM degradation in a murine AAA model. Next, blood samples were collected to separate the serum for detection of inflammatory cytokines. As expected, infusion of Ang II for four weeks elevated serum levels of TNF-α, IL-1β, and IL-6 compared to those in the NS group. However, these changes were reversed by sh-*PVT1* treatment (Fig. 5C).

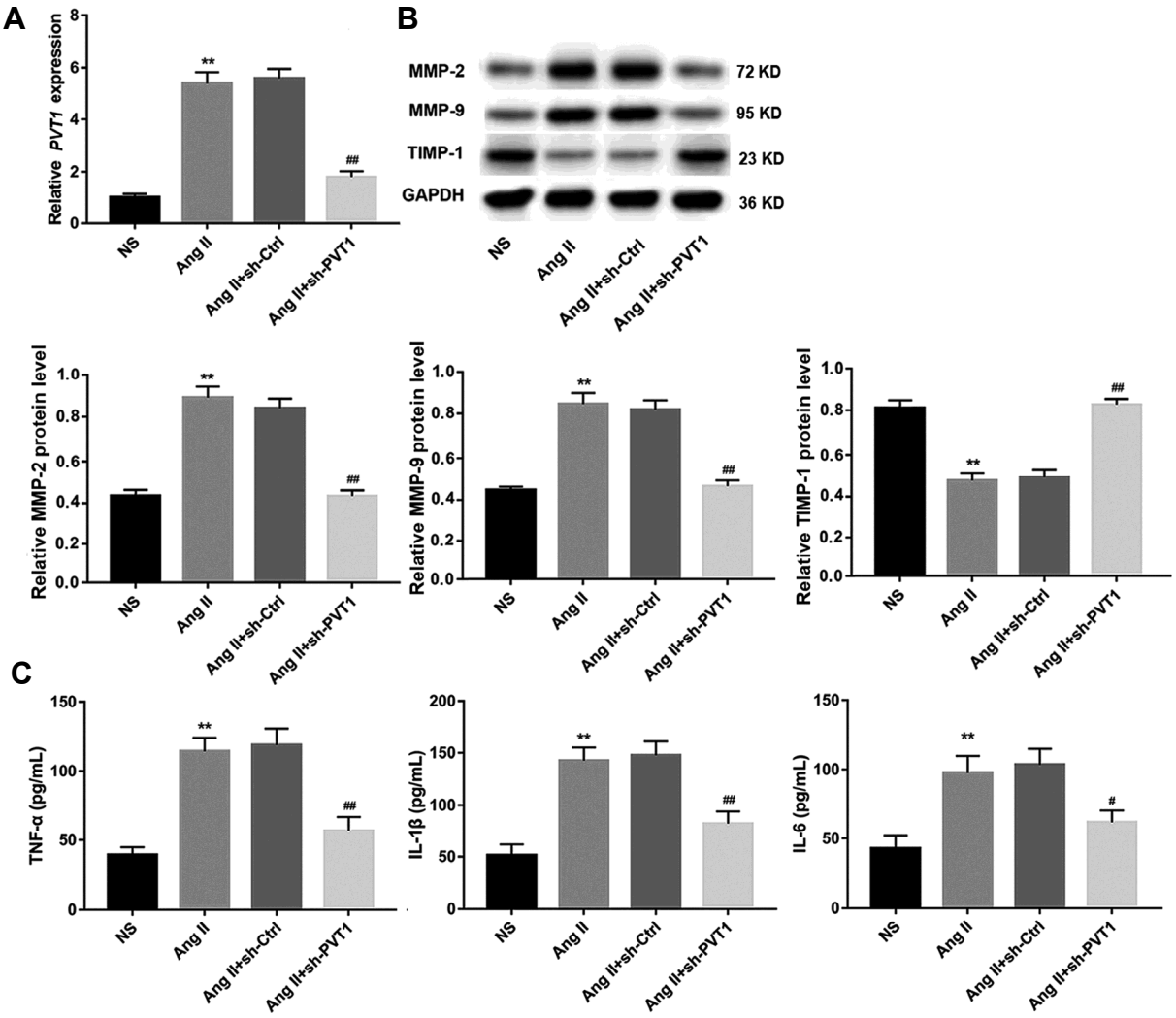

Fig. 5. sh-*PVT1* attenuated Ang II-induced *PVT1* expression, ECM degradation, and inflammation in mice. (A) Relative *PVT1* expression in aortic tissues from mice four weeks after Ang II infusion in each group was examined by qRT-PCR. (B) The protein levels of MMP-2, MMP-9, and TIMP-1 in aortic tissues from mice four weeks after Ang II were examined by Western blot. GAPDH served as the loading control. (C) Four weeks after Ang II infusion, serum levels of the inflammatory cytokines TNF-α, IL-1β, and IL-6 were quantified using ELISA kits. n=15 for each group. $^{**}P < 0.01$ *vs.* NS group, and $^{\#\#}P < 0.01$ *vs.* Ang II+sh-Ctrl group. NS: normal saline; Ang II: Angiotensin II; MMP-2: matrix metalloproteinase-2; MMP-9: matrix metalloproteinase-9; TIMP-1: tissue inhibitors of metalloproteinase-1; TNF-α: tumour necrosis factor-α; IL-1β: interleukin-1β; IL-6: interleukin-6.

DISCUSSION

In the present study, we have shown for the first time that treatment with sh-*PVT1* attenuated the Ang II-induced formation of AAA in ApoE$^{-/-}$ mice by reducing VSMC apoptosis, ECM disruption, and expression of pro-inflammatory cytokines in the serum.

AAA is a vascular disease with a high mortality rate. Due to a lack of effective medications to reverse the progression of AAA, surgery is the most commonly recommended treatment for AAA patients. The phenotypic shift and apoptosis of aortic smooth muscle cells (SMCs), degradation of elastin and collagen, accumulation of T lymphocytes, and neovascularization are the best-known features of AAA (Parvizi and Harmsen, 2015). There are many potential mechanisms involved in the pathogenesis of AAA, including inflammation, VSMCs apoptosis, ECM degradation, and oxidative stress (Wang et al., 2017; Zhang et al., 2018). Pro-inflammatory cytokines such as IL-1β, IL-10, IL-6, IL-13, TNF-α, and interferon (IFN)-γ in the diseased aortic wall promote AAA development by modulating MMP secretion (Parvizi and Harmsen, 2015). MMPs are a family of zinc-dependent endopeptidases that include collagenases and elastases. MMPs mainly target and degrade the components of the ECM, such as collagen and elastin (Diaz et al., 2011). It has been shown that the expression of MMPs is increased in the aortic wall (Morris et al., 2014). MMP activation is tightly regulated by the TIMP family of inhibitors, and downregulation of TIMPs in AAA tissue has also been documented (Defawe et al., 2003; Tamarina et al., 1997). Importantly, the increase in MMPs and decrease in TIMPs contribute to ECM disruption and VSMC apoptosis (Li and Maegdefessel, 2017). Apoptosis of VSMCs leads to the massive loss of these contractile cells and, thus, of dilation of the abdominal aortic wall. Meanwhile, the delicate balance of synthetic and contractile phenotype of SMC is tilted to a synthetic phenotype. In these phenotypically shifted SMCs, ECM turnover is also increased, promoting more ECM degradation than ECM production. Together, these results contribute to AAA progression.

To study the mechanism underlying AAA formation, several animal models have been developed in recent years (Sénémaud et al., 2017). Different animal models for AAA may have diverse pathological manifestations. For example, increased aortic dilation and inflammatory response, which are characterized by medial degeneration with accumulation of macrophages, were observed in a $CaCl_2$-induced AAA model (Chiou et al., 2001). Medial degeneration, accumulation of macrophages and distribution of neutrophils were identified as the pathological characteristics of AAA in an elastase-induced model (Pyo et al., 2000). Indeed, one of the most commonly used mouse models of AAA is Ang II perfusion-induced AAA in ApoE$^{-/-}$ mice, which results in many features similar to those of human lesions, including luminal dilatation, leukocyte infiltration, VSMC apoptosis, and ECM deformation (Qin et al., 2017). In this study, we demonstrated that we successfully established the classical murine Ang II-induced AAA model, as evidenced by aortic dilation, marked adventitial thickening, aortic elastin loss, enhanced aortic cell apoptosis, elevated levels of MMP-2 and MMP-9, reduced levels of TIMP-1, and increased levels of pro-inflammatory cytokines.

Some potential therapeutic drugs have been proposed and tested in animal models and clinical trials, such as statins, angiotensin pathway inhibitors, and antiplatelet drugs (Parvizi and Harmsen, 2015). For example, doxycycline, an inhibitor of MMPs, inhibited the development of AAA in animal experiments (Curci et al., 1998). Macrophage chemotaxis protein-induced protein 3 (MCPIP3) may act as an endogenous inhibitor of the inflammatory signalling pathway in endothelial cells and may be a potential therapeutic target in AAA (Zhang et al., 2018). Gingival fibroblasts help prevent the development of experimental AAA and rupture by promoting TIMP-1 production (Giraud et al., 2017). However, studies on the involvement of lncRNAs in AAA remain scarce (Yang et al., 2016; Zhou et al., 2017).

Yang et al. (Yang et al., 2016) utilized microarray analysis and identified 3,688 lncRNAs that were differently expressed between AAA and normal aortic tissues, in which 1,582 lncRNAs were upregulated and 2,106 lncRNAs were downregulated. Among these lncRNAs, *PVT1* was upregulated more than 3-fold in AAA tissues compared with normal aortic tissue, indicating that *PVT1* is closely related to the pathology of AAA. *PVT1* is a newly discovered lncRNA that functions as an oncogenic molecule in diverse cancer types. For example, overexpression of *PVT1* mimics advanced clinicopathological features and is an unfavourable risk factor for survival of patients with gastrointestinal cancers (Liu et al., 2017). *PVT1* may inhibit paclitaxel-induced epithelial-to-mesenchymal transition and sensitize HPV16-positive CaSki cervical cancer cells to paclitaxel (Shen et al., 2017). Knockdown of *PVT1* enhances the radiosensitivity of NSCLC by sponging miR-195 (Wu et al., 2017). *PVT1* promotes pancreatic cancer cell proliferation and migration by acting as a molecular sponge to regulate miR-448 (Zhao et al., 2018). Despite the extensive investigation concerning *PVT1* in cancer, the role of *PVT1* in AAA has not yet been documented. Recently, Chen et al. (Chen et al., 2017) proposed that, in NSCLC cell lines, *PVT1* facilitated invasion through upregulation of MMP-9, a protein closely related to ECM degradation. In this study, we observed significantly upregulated expression of *PVT1* in abdominal aortic tissues from AAA patients and Ang II-induced AAA model mice, as well as in cultured mouse VSMCs, suggesting an association between *PVT1* expression and AAA. Notably, the effects of Ang II were enhanced by overexpression of *PVT1* but attenuated by knockdown of *PVT1*. These effects included facilitating cell apoptosis, increasing expression of MMP-2 and MMP-9, reducing expression of TIMP-1, and promoting VSMC phenotypic switching from the contractile to synthetic state. Furthermore, knockdown of *PVT1* reversed Ang II-induced AAA formation in mice, as evidenced by attenuation of AAA-associated alterations. These findings confirmed our hypothesis that *PVT1* may facilitate ECM degradation, leading to the apoptosis of VSMCs and the formation of AAA.

Accumulating evidence has demonstrated that *PVT1* functions as an endogenous sponge for certain miRNAs, relieving the inhibitory effects these miRNAs exert on their target

genes. For example, a recent study has shown that *PVT1* promotes the proliferation and migration of pancreatic carcinoma cells by acting as an endogenous sponge for miR-448 to regulate the miRNA target SERBP1 (Wu et al., 2017). *PVT1* can also act as an endogenous sponge for miR-186-5p to reduce its inhibitory effect on yes-associated protein 1 and promote hepatocellular carcinoma tumorigenesis (Lan et al., 2017). Additionally, several miRNAs including miR-218 (Jin et al., 2013), miR-let-7e (Ventayol et al., 2014), miR-127-5p (Tu et al., 2016), and miR-21 (Wang et al., 2013) can target MMP-2, MMP-9, TIMP-1, or OPN. Therefore, we speculate that *PVT1* may serve as a sponge for certain miRNAs that target AAA-related genes such as MMP-2, MMP-9, TIMP-1, or OPN. Although this hypothesis requires further investigation, such a mechanism may explain the role of *PVT1* in AAA.

In summary, we have shown in the present study that sh-*PVT1* treatment attenuated Ang II-induced formation of AAA in association with a reduction in VSMC apoptosis, ECM disruption, and serum pro-inflammatory cytokines. Inhibition of lncRNA *PVT1* may be a novel strategy for preventing the progression of AAA.

REFERENCES

Ailawadi, G., Moehle, C., Pei, H., Walton, S., Yang, Z., Kron, I., Lau, C., and Owens, G. (2009). Smooth muscle phenotypic modulation is an early event in aortic aneurysms. J. Thorac. Cardiovasc. Surg. *138*, 1392-1399.

Chen, W., Zhu, H., Yin, L., Wang, T., Wu, J., Xu, J., Tao, H., Liu, J., and He, X. (2017). lncRNA-PVT1 facilitates invasion through upregulation of MMP9 in nonsmall cell lung cancer cell. DNA Cell Bio. *36*, 787-793.

Chiou, A.C., Chiu, B., and Pearce, W.H. (2001). Murine aortic aneurysm produced by periarterial application of calcium chloride. J. Surg. Res. *99*, 371-376.

Curci, J.A., Petrinec, D., Liao, S., Golub, L.M., and Thompson, R.W. (1998). Pharmacologic suppression of experimental abdominal aortic aneurysms: acomparison of doxycycline and four chemically modified tetracyclines. J. Vasc. Surg. *28*, 1082-1093.

Defawe, O.D., Colige, A., Lambert, C.A., Munaut, C., Delvenne, P., Lapiere, C.M., Limet, R., Nusgens, B.V., and Sakalihasan, N. (2003). TIMP-2 and PAI-1 mRNA levels are lower in aneurysmal as compared to athero-occlusive abdominal aortas. Cardiovasc. Res. *60*, 205-213.

Diaz, A., Garcia, F., Mozos, A., Caballero, M., Leon, A., Martinez, A., Gil, C., Plana, M., Gallart, T., Gatell, J.M., et al. (2011). Lymphoid tissue collagen deposition in HIV-infected patients correlates with the imbalance between matrix metalloproteinases and their inhibitors. J. Infect. Dis. *203*, 810-813.

Freestone, T., Turner, R.J., Coady, A., Higman, D.J., Greenhalgh, R.M., and Powell, J.T. (1995). Inflammation and matrix metalloproteinases in the enlarging abdominal aortic aneurysm. Arterioscler. Thromb. Vasc. Biol. *15*, 1145-1151.

Fu, X.M., Yamawaki-Ogata, A., Oshima, H., Ueda, Y., Usui, A., and Narita, Y. (2013). Intravenous administration of mesenchymal stem cells prevents angiotensin II-induced aortic aneurysm formation in apolipoprotein E-deficient mouse. J. Transl. Med. *11*, 175.

Galis, Z.S., Muszynski, M., Sukhova, G.K., Simon-Morrissey, E., and Libby, P. (1995). Enhanced expression of vascular matrix metalloproteinases induced *in vitro* by cytokines and in regions of human atherosclerotic lesions. Ann. NY. Acad. Sci. *748*, 501-507.

Giraud, A., Zeboudj, L., Vandestienne, M., Joffre, J., Esposito, B., Potteaux, S., Vilar, J., Cabuzu, D., Kluwe, J., Seguier, S., et al. (2017). Gingival fibroblasts protect against experimental abdominal aortic aneurysm development and rupture through tissue inhibitor of metalloproteinase-1 production. Cardiovasc. Res. *113*, 1364-1375.

Guo, D., Wang, Y., Ren, K., and Han, X. (2018). Knockdown of LncRNA PVT1 inhibits tumorigenesis in non-small-cell lung cancer by regulating miR-497 expression. Exp. Cell Res. *362*, 172-179.

Jin, J., Cai, L., Liu, Z.M., and Zhou, X.S. (2013). miRNA-218 inhibits osteosarcoma cell migration and invasion by down-regulating of TIAM1, MMP2 and MMP9. Asian Pac. J. Cancer Prev. *14*, 3681-3684.

Kent, K.C. (2014). Clinical practice. Abdominal aortic aneurysms. N. Engl. J. Med. *371*, 2101-2108.

Kosmala, W., Plaksej, R., Przewlocka-Kosmala, M., Kuliczkowska-Plaksej, J., Bednarek-Tupikowska, G., and Mazurek, W. (2008). Matrix metalloproteinases 2 and 9 and their tissue inhibitors 1 and 2 in premenopausal obese women: relationship to cardiac function. Int. J. Obes. *32*, 763-771.

Kumar, Y., Hooda, K., Li, S., Goyal, P., Gupta, N., and Adeb, M. (2017). Abdominal aortic aneurysm: pictorial review of common appearances and complications. Ann. Transl. Med. *5*, 256.

Kung, J.T., Colognori, D., and Lee, J.T. (2013). Long noncoding RNAs: past, present, and future. Genetics *193*, 651-669.

Lan, T., Yan, X., Li, Z., Xu, X., Mao, Q., Ma, W., Hong, Z., Chen, X., and Yuan, Y. (2017). Long non-coding RNA PVT1 serves as a competing endogenous RNA for miR-186-5p to promote the tumorigenesis and metastasis of hepatocellular carcinoma. Tumour Biol. *39*, 1010428317705338.

Li, Y., and Maegdefessel, L. (2017). Non-coding RNA contribution to thoracic and abdominal aortic aneurysm disease development and progression. Front. Physiol. *8*, 429.

Liu, F., Dong, Q., and Huang, J. (2017). Overexpression of LncRNA PVT1 predicts advanced clinicopathological features and serves as an unfavorable risk factor for survival of patients with gastrointestinal cancers. Cell Physiol. Biochem. *43*, 1077-1089.

Maegdefessel, L., Azuma, J., Toh, R., Merk, D.R., Deng, A., Chin, J.T., Raaz, U., Schoelmerich, A.M., Raiesdana, A., Leeper, N.J., et al. (2012). Inhibition of microRNA-29b reduces murine abdominal aortic aneurysm development. J. Clin. Invest. *122*, 497-506.

Martorell, S., Hueso, L., Gonzalez-Navarro, H., Collado, A., Sanz, M., and Piqueras, L. (2016). Vitamin D receptor activation reduces angiotensin-II-induced dissecting abdominal aortic aneurysm in apolipoprotein E-knockout mice. Arterioscler. Thromb. Vasc. Biol. *36*, 1587-1597.

Miyake, T., and Morishita, R. (2009). Pharmacological treatment of abdominal aortic aneurysm. Cardiovasc. Res. *83*, 436-443.

Morris, D.R., Biros, E., Cronin, O., Kuivaniemi, H., and Golledge, J. (2014). The association of genetic variants of matrix metalloproteinases with abdominal aortic aneurysm: a systematic review and meta-analysis. Heart *100*, 295-302.

Ng, S.Y., Lin, L., Soh, B.S., and Stanton, L.W. (2013). Long noncoding RNAs in development and disease of the central nervous system. Trends Genet. *29*, 461-468.

Pande, R.L., and Beckman, J.A. (2008). Abdominal aortic aneurysm: populations at risk and how to screen. J. Vasc. Interv. Radiol. *19*, S2-8.

Parvizi, M., and Harmsen, M. (2015). Therapeutic prospect of adipose-derived stromal cells for the treatment of abdominal aortic aneurysm. Stem Cells Dev. *24*, 1493-1505.

Pyo, R., Lee, J.K., Shipley, J.M., Curci, J.A., Mao, D., Ziporin, S.J., Ennis, T.L., Shapiro, S.D., Senior, R.M., and Thompson, R.W. (2000). Targeted gene disruption of matrix metalloproteinase-9 (gelatinase B)

suppresses development of experimental abdominal aortic aneurysms. J. Clin. Invest. *105*, 1641-1649.

Qin, Y., Wang, Y., Liu, O., Jia, L., Fang, W., Du, J., and Wei, Y. (2017). Tauroursodeoxycholic acid attenuates angiotensin II induced abdominal aortic aneurysm formation in apolipoprotein E-deficient mice by inhibiting endoplasmic reticulum stress. Eur. J. Vasc. Endovasc. Surg. *53*, 337-345.

Ren, H., Li, F., Tian, C., Nie, H., Wang, L., Li, H.H., and Zheng, Y. (2015). Inhibition of proteasome activity by low-dose bortezomib attenuates angiotensin II-induced abdominal aortic aneurysm in apo E(-/-) mice. Sci. Rep. *5*, 15730.

Sénémaud, J., Caligiuri, G., Etienne, H., Delbosc, S., Michel, J., and Coscas, R. (2017). Translational relevance and recent advances of animal models of abdominal aortic aneurysm. Arterioscler. Thromb. Vasc. Biol. *37*, 401-410.

Sachdeva, J., Mahajan, A., Cheng, J., Baeten, J.T., Lilly, B., Kuivaniemi, H., and Hans, C.P. (2017). Smooth muscle cell-specific Notch1 haploinsufficiency restricts the progression of abdominal aortic aneurysm by modulating CTGF expression. PLoS One *12*, e0178538.

Sakata, K., Shigemasa, K., Nagai, N., and Ohama, K. (2000). Expression of matrix metalloproteinases (MMP-2, MMP-9, MT1-MMP) and their inhibitors (TIMP-1, TIMP-2) in common epithelial tumors of the ovary. Int. J. Oncol. *17*, 673-681.

Shen, C.J., Cheng, Y.M., and Wang, C.L. (2017). LncRNA PVT1 epigenetically silences miR-195 and modulates EMT and chemoresistance in cervical cancer cells. J. Drug Target. *25*, 637-644.

Tamarina, N.A., McMillan, W.D., Shively, V.P., and Pearce, W.H. (1997). Expression of matrix metalloproteinases and their inhibitors in aneurysms and normal aorta. Surgery *122*, 264-271.

Tu, M., Li, Y., Zeng, C., Deng, Z., Gao, S., Xiao, W., Luo, W., Jiang, W., Li, L., and Lei, G. (2016). MicroRNA-127-5p regulates osteopontin expression and osteopontin-mediated proliferation of human chondrocytes. Sci. Rep. *6*, 25032.

Ventayol, M., Viñas, J.L., Sola, A., Jung, M., Brüne, B., Pi, F., Mastora, C., and Hotter, G. (2014). miRNA let-7e targeting MMP9 is involved in adipose-derived stem cell differentiation toward epithelia. Cell Death Dis. *5*, e1048.

Wang, J., Gao, Y., Ma, M., Li, M., Zou, D., Yang, J., Zhu, Z., and Zhao, X. (2013). Effect of miR-21 on renal fibrosis by regulating MMP-9 and TIMP1 in kk-ay diabetic nephropathy mice. Cell Biochem. Biophys. *67*, 537-546.

Wang, S., Xie, J., Green, L., McCready, R., Motaganahalli, R., Fajardo, A., Babbey, C., and Murphy, M. (2017). TSG-6 is highly expressed in human abdominal aortic aneurysms. J. Surg. Res. *220*, 311-319.

Watanabe, A., Ichiki, T., Sankoda, C., Takahara, Y., Ikeda, J., Inoue, E., Tokunou, T., Kitamoto, S., and Sunagawa, K. (2014). Suppression of abdominal aortic aneurysm formation by inhibition of prolyl hydroxylase domain protein through attenuation of inflammation and extracellular matrix disruption. Clin. Sci. *126*, 671-678.

Wu, D., Li, Y., Zhang, H., and Hu, X. (2017). Knockdown of lncrna PVT1 enhances radiosensitivity in non-small cell lung cancer by sponging mir-195. Cell Physiol. Biochem. *42*, 2453-2466.

Yang, Y.G., Li, M.X., Kou, L., Zhou, Y., Qin, Y.W., Liu, X.J., and Chen, Z. (2016). Long noncoding RNA expression signatures of abdominal aortic aneurysm revealed by microarray. Biomed. Environ. Sci. *29*, 713-723.

Zhang, S., Du, X., Chen, Y., Tan, Y., and Liu, L. (2018). Potential medication treatment according to pathological mechanisms in abdominal aortic aneurysm. J. Cardiovasc. Pharmacol. *71*, 46-57

Zhao, L., Kong, H., Sun, H., Chen, Z., Chen, B., and Zhou, M. (2018). LncRNA-PVT1 promotes pancreatic cancer cells proliferation and migration through acting as a molecular sponge to regulate miR-448. J. Cell. Physiol. *233*, 4044-4055

Zhou, Y., Wang, J., Xue, Y., Fang, A., Wu, S., Huang, K., Tao, L., Wang, J., Shen, Y., Wang, J., et al. (2017). Microarray analysis reveals a potential role of lncRNA expression in 3,4-benzopyrene/angiotensin II-activated macrophage in abdominal aortic aneurysm. Stem Cells Int. *2017*, 9495739.